Computing, Telecommunication and Control, 2024, Vol. 17, No. 4, Pp. 46–55.
Информатика, телекоммуникации и управление. 2024. Том 17, № 4. С. 46–55.

Research article
DOI: https://doi.org/10.18721/JCSTCS.17404
UDC 621.3.049.774.2

CHANNEL SELECTION AT INPUT OF NARROWBAND DIRECT-CONVERSION RECEIVER BASED ON CURRENT-DRIVEN PASSIVE MIXER

T.D. Tran ✉

Peter the Great St. Petersburg Polytechnic University,
St. Petersburg, Russian Federation

✉ thanhdat140495@gmail.com

Abstract. Some issues when applying a Miller N-path filter to narrowband direct-conversion receiver (DCR) based on current-driven passive mixer and solutions to mitigate those issues are presented. The small impedances of the parallel LC circuit of low noise amplifier (LNA) at high frequencies cause undesirable effects: conversion gain reduction, noise figure increase and non-linear effects of the switches. A commutated network with the addition of resistors R_{FB1} and R_{FB2} is proposed to reduce the influence of those undesirable effects. The receiver is designed in the frequency range from 2.4 GHz to 2.6 GHz with 0.18 μm CMOS UMC technology. When applying the Miller N-path filter, although the conversion gain decreased by 3 dB and the noise figure increased by 1 dB, the in-band linearity (P_{1dB} and IIP3) of the DRC increased by 6–9 dB compared to the DRC without the Miller N-path filter.

Keywords: narrowband direct-conversion receiver, current-driven passive mixer, Miller N-path filter, channel selection, low noise amplifier, commutated network

Citation: Tran T.D. Channel selection at input of narrowband direct-conversion receiver based on current-driven passive mixer. Computing, Telecommunications and Control, 2024, Vol. 17, No. 4, Pp. 46–55. DOI: 10.18721/JCSTCS.17404

Научная статья
DOI: https://doi.org/10.18721/JCSTCS.17404
УДК 621.3.049.774.2

КАНАЛЬНАЯ ФИЛЬТРАЦИЯ НА ВХОДЕ УЗКОПОЛОСНОГО ПРИЕМНИКА ПРЯМОГО ПРЕОБРАЗОВАНИЯ НА ОСНОВЕ ПАССИВНОГО СМЕСИТЕЛЯ С УПРАВЛЕНИЕМ ПО ТОКУ

Т.Д. Чан ✉

Санкт-Петербургский политехнический университет Петра Великого,
Санкт-Петербург, Российская Федерация

✉ thanhdat140495@gmail.com

Аннотация. В статье рассмотрены некоторые проблемы, возникающие при применении N-канального фильтра Миллера в узкополосном приемнике прямого преобразования (ППП) на основе пассивного смесителя с управлением по току, а также методы устранения этих проблем. Малые импедансы параллельного LC-контура малошумящего усилителя (МШУ) на высоких частотах приводят к таким нежелательным последствиям, как снижение коэффициента передачи, увеличение коэффициента шума и нелинейные эффекты в переключателях. Для уменьшения влияния этих нежелательных последствий предлагается коммутируемая схема с добавлением резисторов R_{FB1} и R_{FB2}. Приемник предназначен для работы в диапазоне частот от 2,4 ГГц до 2,6 ГГц с использованием 0,18 мкм КМОП-технологии компании UMC. При применении N-канального фильтра Миллера, хотя коэффициент передачи снизился на 3 дБ, а коэффициент шума увеличился на 1 дБ, внутриполосная линейность (P_{1dB} и IIP3) ППП увеличилась на 6–9 дБ по сравнению с приемником без применения N-канального фильтра Миллера.

Ключевые слова: узкополосный приемник прямого преобразования, пассивный смеситель с управлением по току, N-канальный фильтр Миллера, канальная фильтрация, малошумящий усилитель, коммутируемая схема

Для цитирования: Tran T.D. Channel selection at input of narrowband direct-conversion receiver based on current-driven passive mixer // Computing, Telecommunications and Control. 2024. Т. 17, № 4. С. 46–55. DOI: 10.18721/JCSTCS.17404

Introduction

Current-driven passive mixer is a suitable choice for modern direct-conversion receivers (DCR), because it has low flicker noise and high linearity [1–8]. For narrowband DRC based on current-driven passive mixer, to achieve the maximum conversion gain of the receiver, the coupling capacitor needs to be nearly resonant with the inductor at the load of the low noise amplifier (LNA) [9–11]. This resonance not only suppresses out-of-band interferers, but also eliminates noise at the harmonics of local oscillator (LO) frequency that are not down-converted to the baseband at the mixer output, significantly reducing the noise figure of the receiver.

However, the large conversion gain of the receiver reduces its linearity. In practice, the 1 dB compression point (P_{1dB}) and input third-order intercept point (IIP3) of the receiver are in the ranges of −26 dBm to −23 dBm and −14 dBm to −10 dBm, respectively. With such a low level of linearity, the conversion gain of the receiver will be drastically reduced when receiving in-band interference of not very high power, such as −15 dBm. To suppress in-band interferences the Miller N-path filter was used as a channel selection filter. In these papers, LNA is designed to work over a wide frequency range [12–16]. Therefore, its output impedance is a resistance. On the other hand, for narrowband DCR based on current-driven passive mixer, the LNA loads a parallel LC circuit. Therefore, when applying a Miller N-path filter to this receiver, some issues appear, such as conversion gain reduction, noise figure increase and non-linear effects of switches.

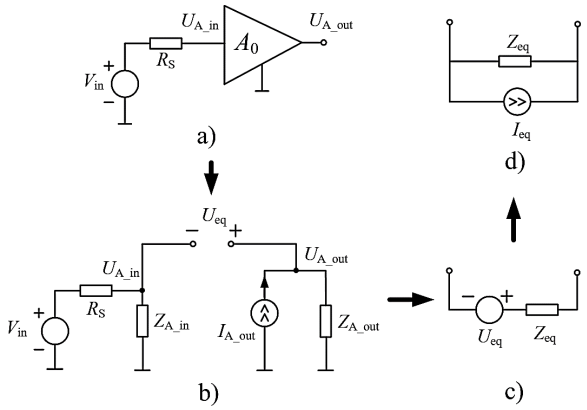

Fig. 1. LNA circuit with input source (a), equivalent circuit of LNA with input source (b), equivalent source between the input and output nodes of the LNA (Thevenin equivalent) (c, d)

This paper studies some issues when applying a Miller N-path filter to narrowband DCR based on current-driven passive mixer and proposes solutions to mitigate those issues.

Some issues applying a Miller *N*-path filter to narrowband DCR based on current-driven passive mixer

When applying a Miller N-path filter to a narrowband DCR, it is necessary to connect a commutated network between the input and output nodes of the LNA as shown in [13]. Using Thevenin equivalent LNA together with input voltage source $V_{in}(\omega)$ (Fig. 1a) and its impedance $R_S = 50$ Ohm is equivalent to a circuit consisting of a voltage source $U_{eq}(\omega)$ connected in series with impedance $Z_{eq}(j\omega)$ (Fig. 1c) or a current source $I_{eq}(\omega)$ in parallel with impedance $Z_{eq}(j\omega)$ (Fig. 1d) calculated by the following formulas:

$$U_{eq}(\omega) = \frac{Z_{A\_in}(j\omega)V_{in}(\omega)\left[A_0(j\omega)-1\right]}{Z_{A\_in}(j\omega)+R_S},$$

$$Z_{eq}(j\omega) = \frac{Z_{A\_in}(j\omega)R_S\left[1-A_0(j\omega)\right]}{Z_{A\_in}(j\omega)+R_S} + Z_{A\_out}(j\omega), \qquad (1)$$

$$I_{eq}(\omega) = \frac{U_{eq}(\omega)}{Z_{eq}(j\omega)},$$

where $Z_{A\_in}(j\omega)$, $Z_{A\_out}(j\omega)$ are input and output impedances of the LNA, respectively; $A_0(j\omega)$ is the conversion gain of the LNA.

Then, when connecting the commutated network to the input and output nodes of the LNA, we obtain the circuit for the small-signal model in Fig. 2. Using the methodology presented in [17], the current $I_{in1}(\omega)$ is calculated. Then, at $0.8\omega_c < \omega < 1.2\omega_c$, where ω_c is the switching angular frequency, the voltage $U_{eq1}(\omega)$ is calculated by the formula:

$$U_{eq1}(\omega) = \left[I_{eq}(\omega) - I_{in1}(\omega)\right]Z_{eq}(j\omega) =$$
$$= \left[R_{SW} + Z_{CL}(j\omega) + \frac{c(\omega)Z_{eq}(j\omega)}{(1+g(\omega))Z(j\omega)}\right]\frac{I_{eq}(\omega)Z_{eq}(j\omega)}{Z(j\omega)} \approx \left[R_{SW} + \frac{c(\omega)}{1+g(\omega)}\right]I_{eq}(\omega), \qquad (2)$$

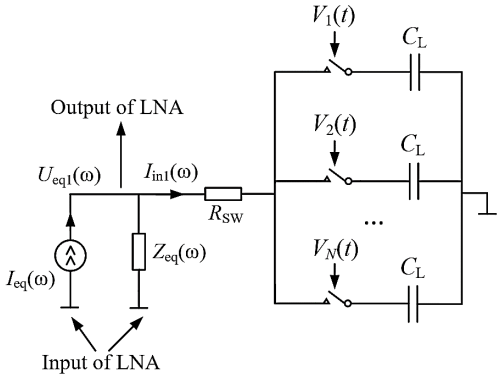

Fig. 2. Equivalent circuit for the small-signal model
when connecting a commutated network to the input and output nodes of the LNA

$$\text{where } c(\omega)=\frac{N\sin\left(\left(\pi-\frac{\pi}{N}\right)\frac{\omega}{\omega_c}\right)\sin\left(\frac{\pi\omega}{N\omega_c}\right)Z_{CL}(j\omega_c)}{2\pi\sin\left(\left(\frac{\omega-\omega_c}{\omega_c}\right)\pi\right)},\ g(\omega)=\sum_{l=-\infty}^{+\infty}\frac{c(\omega)}{(1+lN)^2 Z(j\omega+lNj\omega_c)},$$

$$Z(j\omega)=Z_{eq}(j\omega)+R_{SW}+Z_{CL}(j\omega)\approx Z_{eq}(j\omega),\ Z_{CL}(j\omega)=\frac{1}{j\omega C_L}.$$

Firstly, let us consider the conversion gain reduction of the LNA. Now we calculate the output voltage $|U_{eq1}(\omega)|$ of the LNA for the desired signal at the frequency $\omega \approx \omega_c$. In this case, the ratio $(\omega - \omega_c)/\omega_c \approx 0$, therefore $|c(\omega)| >> |Z_{eq}(j\omega)| \approx |Z(j\omega)|$. Then formula (2) will take the form:

$$U_{eq1}(\omega)=\left[R_{SW}+\frac{1}{\sum_{l=-\infty}^{+\infty}\frac{1}{(1+lN)^2 Z_{eq}(j\omega+lNj\omega_c)}}\right]I_{eq}(\omega)\approx\frac{I_{eq}(\omega)}{\sum_{l=-\infty}^{+\infty}\frac{1}{(1+lN)^2 Z_{eq}(j\omega+lNj\omega_c)}},$$

taking into account the following approximation:

$$R_{SW}<<\left|\frac{1}{\sum_{l=-\infty}^{+\infty}\frac{1}{(1+lN)^2 Z_{eq}(j\omega+lNj\omega_c)}}\right|.$$

As mentioned above [12–16], $Z_{eq}(j\omega)$ is a resistor over a wide frequency range. Then we have:

$$U_{eq1}(\omega)=\frac{I_{eq}(\omega)}{\sum_{l=-\infty}^{+\infty}\frac{1}{(1+lN)^2 Z_{eq}(j\omega+lNj\omega_c)}}\approx\frac{I_{eq}(\omega)}{\frac{1}{Z_{eq}(j\omega)}}=I_{eq}(\omega)Z_{eq}(j\omega)=U_{eq}(\omega).$$

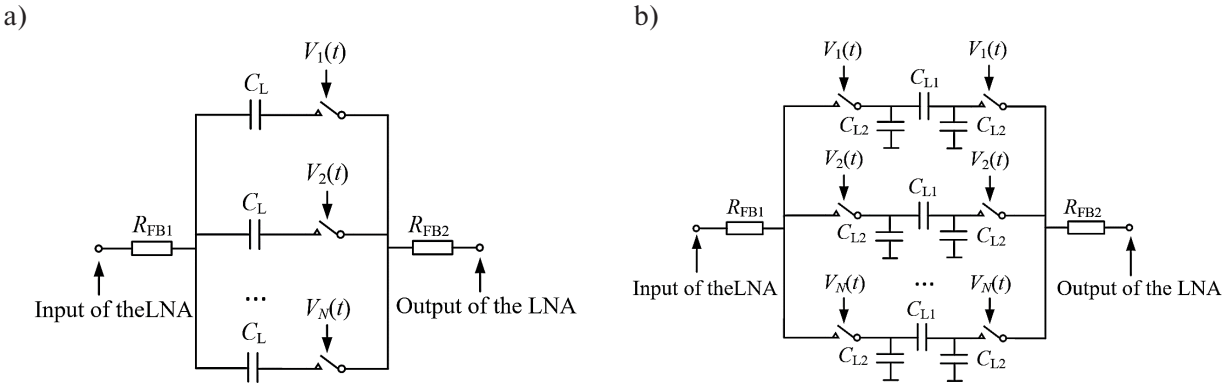

Fig. 3. Commutated network with resistors R_{FB1} and R_{FB2} (a); commutated network with increased filtering efficiency (b)

This means that the output voltage $|U_{eq1}(\omega)|$ of the LNA with the commutated network for the desired signal at frequency ω is approximately equal to the output voltage $|U_{eq}(\omega)|$ of the LNA without the commutated network for the desired signal at frequency ω. On the other hand, in a narrowband DCR based on current-driven passive mixer, $|A_0(j\omega)|$ and $|Z_{A\_out}(j\omega)|$ are large only near the input frequency f_{in} and are very small at high frequencies due to the selectivity of the parallel LC circuit at the output of the LNA. Therefore, from (1) it is clear that $|Z_{eq}(j\omega)|$ is large only near the input frequency f_{in} and is very small at high frequencies. Consequently, it is impossible to apply the following approximation:

$$U_{eq1}(\omega) = \frac{I_{eq}(\omega)}{\sum\limits_{l=-\infty}^{+\infty} \frac{1}{(1+lN)^2 Z_{eq}(j\omega + lNj\omega_c)}} \approx \frac{I_{eq}(\omega)}{\frac{1}{Z_{eq}(\omega)}}.$$

Then, small values of $|Z_{eq}(j\omega + lNj\omega_c)|$ at high frequencies will significantly reduce $|U_{eq1}(\omega)|$. Consequently, the conversion gain of the LNA and receiver decreases.

Secondly, consider the noise figure increase of the LNA and receiver. Due to the conversion gain reduction of the LNA, the noise contribution of the LNA noise sources, the mixer, and subsequent stages will increase significantly, increasing the noise figure of the LNA and receiver.

Thirdly, when connecting transistors (switches) of the commutated network directly between the input and output nodes of the LNA, the voltage level at the transistor terminal is quite high, which causes nonlinear effects of the transistors.

Solutions to mitigate indicated issues

The reason for the conversion gain reduction and the noise figure increase of the narrowband DCR based on current-driven passive mixer is that $|Z_{eq}(j\omega)|$ has very small values at high frequencies. To reduce these undesirable effects, it is necessary to increase $|Z_{eq}(j\omega)|$ at high frequencies. For this purpose, resistors R_{FB1} and R_{FB2} are introduced, as shown in Fig. 3a. To further increase the filtering efficiency, a commutated network is used in [13], which is shown in Fig. 3b with the resistors R_{FB1} and R_{FB2}.

In addition, the resistor R_{FB2} isolates the terminal of the transistors (switches) of the commutated network from the output of the LNA, thereby reducing the voltage level at this terminal of the transistors and not causing nonlinear effects.

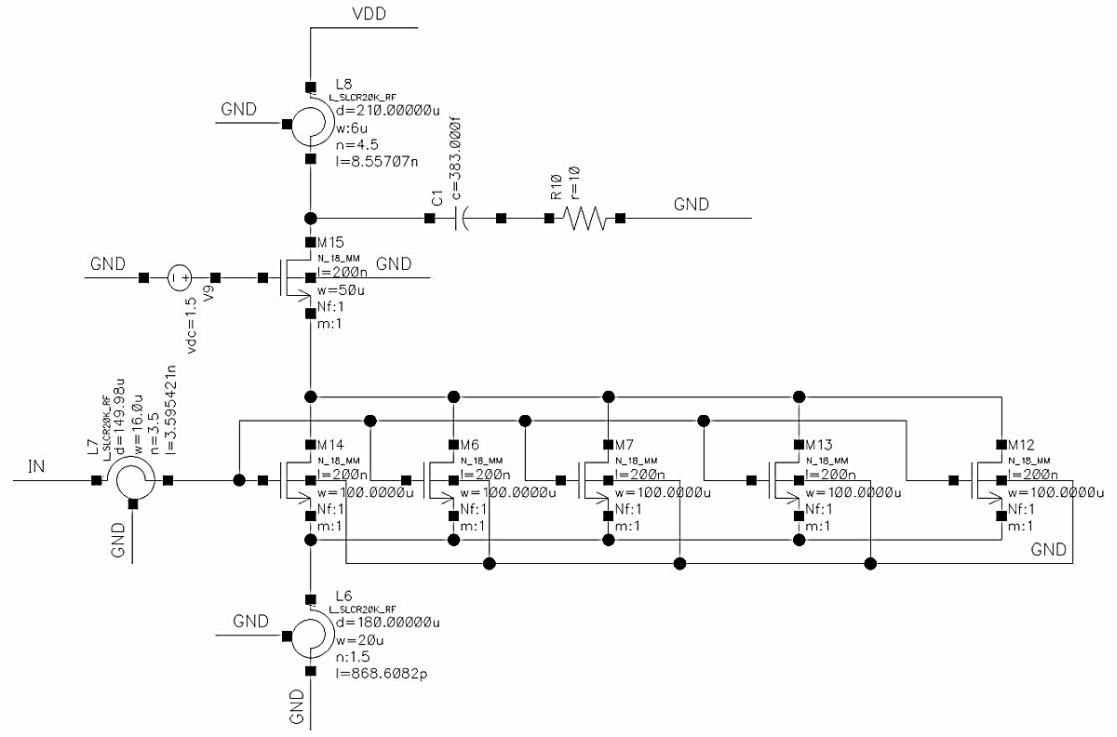

Fig. 4. The schematic of the LNA

Design of narrowband DCR based on current-driven passive mixer

The schematic of the narrowband DCR based on current-driven passive mixer is presented in [9]. The receiver is designed in the frequency range from 2.4 GHz to 2.6 GHz (desired frequency band) with 0.18 μm CMOS UMC technology. Fig. 4 shows the schematic of the LNA based on inductively-degenerated cascode common-source topology [18]. In this circuit, C is the coupling capacitor between the LNA and the mixer and is calculated using the method in [9]. The resistor R = 10 Ohm at the output of the LNA is the input impedance of the subsequent stages: mixer and transimpedance amplifier (TIA). This resistance needs to be small enough to ensure the switches work in current mode and not worsen the quality factor of the inductor L of the LNA. In the desired frequency band, the performances of LNA according to simulation results are: $|A_0|$ = 22.3 dB; noise figure NF = 2.1 dB; transconductance G = = 77.5 mA/V, which is determined by the ratio of the current flowing through the coupling capacitor C to the input voltage V_{in} of the LNA.

The schematic of the TIA is shown in Fig. 5. The TIA is designed using a common gate circuit to ensure its minimum input impedance. According to the simulation results, its input impedance is a parallel RC-circuit with R_{BB} = 82 Ohm and C_{BB} = 20 pF.

The width W_{mix} of the transistors (switches) of the current-driven passive mixer is chosen so that its resistance R_{SW} is small enough and its parasitic capacitance does not significantly reduce the conversion gain of the receiver. The optimal value is W_{mix} = 120 μm with "the number of fingers" being two. Then R_{SW} = 5 Ohm.

Simulation results when applying Miller *N*-path filter

The LNA circuit with the commutated network in Fig. 3b when $C_{L1} = C_{L2}$ = 2 pF was simulated using the Cadence software platform for the 0.18 μm CMOS UMC technology. For a fixed width W = 10 μm with "the number of fingers" being one of the switches, the dependence of the LNA performances on R_{FB1} and R_{FB2} is presented in Table 1.

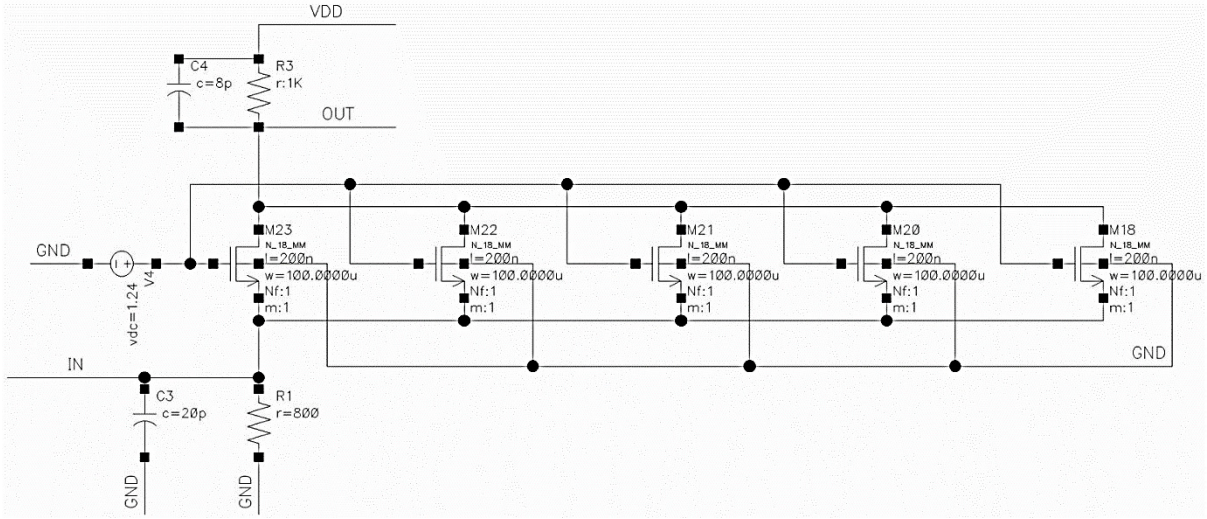

Fig. 5. Schematic of the TIA

Table 1

Dependence of the LNA performances on R_{FB1} and R_{FB2}

R_{FB1}, Ohm	0	50	100	200	200	300
R_{FB2}, Ohm	0	150	300	400	600	700
G, mA/V	32.1	52.2	58.8	60.9	63.5	64
K_S, dB	16.8	11.2	7.9	6.3	5.2	4.3
NF, dB	3.40	3.03	2.86	2.70	2.69	2.61

where K_S is the in-band interference suppression coefficient, which is determined by the ratio transconductance G of the LNA for the desired signal to G for in-band interference; NF is the noise figure of the LNA.

The simulation results in Table 1 show that when resistors R_{FB1} and R_{FB2} are absent, although high in-band interference suppression K_S = 16.8 dB is achieved, the transconductance G and noise figure NF of the LNA are deteriorated by 7.7 dB and 1.3 dB compared to the case without the commutated network. With an increase in R_{FB1} and R_{FB2} causing $|Z_{eq}(j\omega)|$ to increase at high frequencies, these deteriorations are reduced. For R_{FB1} = 200 Ohm and R_{FB2} = 400 Ohm, the dependence of the LNA performances on the width W with "the number of fingers" being one of the switches is presented in Table 2.

Table 2

Dependence of LNA performances on the width W of the switches when R_{FB1} = 200 Ohm and R_{FB2} = 400 Ohm

W, μm	2	5	10	15	20	30
G, mA/V	71	66.5	60.9	56.5	53	47.7
K, dB	5.2	6.3	6.3	5.9	5.5	4.8
NF, dB	2.34	2.52	2.70	2.85	2.97	3.17

The simulation results in Table 2 show that with increasing width W of the switches the transconductance G and noise figure NF of the LNA deteriorate due to the increase in the total parasitic capacitance of the switches. Since these parasitic capacitances reduce $|Z_{A\_in}(j\omega)|$ and $|Z_{A\_out}(j\omega)|$ (and consequently

$|Z_{eq}(j\omega)|$) at high frequencies. Based on the simulation result in Tables 1 and 2, W = 10 μm with "the number of fingers" being one, R_{FB1} = 200 Ohm and R_{FB2} = 400 Ohm are selected. In this case, the simulation results of the LNA show that although the conversion gain and the noise figure of the LNA are deteriorated by 2.1 dB and 0.6 dB, respectively, its linearity increased by 8–10 dB.

The narrowband DCR based on current-driven passive mixer was simulated with R_{SW} = 5 Ohm for two cases: with and without commutated network. Its performances are shown in Table 3.

Table 3

Performances of DCR

	DRC with commutated network	**DRC without commutated network**
K_G, dB	23.5	26.5
NF, dB	3.42	2.45
P_{1dB}, dBm	from –14 to –10	from –20 to –18.5
IIP3, dBm	from –1 to +3	from –9 to –4

where KG is the conversion gain of the DRC, which is calculated by the ratio of the differential output voltage of DRC to its input voltage.

The simulation results in Table 3 indicate that when using commutated network (applying Miller N-path filter), although the conversion gain K_G decreased by 3 dB and the noise figure NF increased by 1 dB, the in-band linearity (P_{1dB} and IIP3) of the DRC increased by 6–9 dB compared to the DRC without commutated network.

Conclusion

The issues when applying a Miller N-path filter to narrowband DCR based on current-driven passive mixer are considered: conversion gain reduction, noise figure increase and non-linear effects of switches. The reason for these issues lies in the small impedances of the parallel LC circuit at high frequencies. Due to these imperfections, when using the commutated network, the conversion gain and the noise figure of the LNA are deteriorated by 7.7 dB and 1.3 dB, respectively. A commutated network with the addition of resistors R_{FB1} and R_{FB2} is proposed to reduce the influence of imperfections. Based on the simulation result, W = 10 μm with "the number of fingers" being one, R_{FB1} = 200 Ohm and R_{FB2} = 400 Ohm are selected. When using commutated network, although the conversion gain decreased by 3 dB and the noise figure increased by 1 dB, the in-band linearity (P_{1dB} and IIP3) of the DRC increased by 6–9 dB compared to the DRC without commutated network.

REFERENCES

1. **Sosio M., Liscidini A., Castello R.** An intuitive current-driven passive mixer model based on switched-capacitor theory. IEEE Transactions on Circuits and Systems II: Express Briefs, 2013, Vol. 60, No. 2, Pp. 66–70. DOI: 10.1109/TCSII.2012.2234993

2. **Naseh N., Bardeh M.G., Entesari K.** A signal generator and down-conversion mixer / TIA unit for a 5.8-GHz FMCW receiver in 65nm CMOS. 2023 IEEE Radio and Wireless Symposium (RWS), 2023, Pp. 70–72. DOI: 10.1109/RWS55624.2023.10046310

3. **Korotkov A.S., Tran T.D.** A method for analysis of current-driven passive mixer with considering arbitrary input impedance and time constant of RC-load. 2022 International Conference on Electrical Engineering and Photonics (EExPolytech), 2022, Pp. 21–24. DOI: 10.1109/EExPolytech56308.2022.9950911

4. **Elsayed O., Zarate-Roldan J., Abuellil A., Hussien F.A.-L., Eladawy A., Sánchez-Sinencio E.** Highly linear low-power wireless RF receiver for WSN. IEEE Transactions on Very Large Scale Integration (VLSI) Systems, 2019, Vol. 27, No. 5, Pp. 1007–1016. DOI: 10.1109/TVLSI.2018.2890093

5. **Gebhard A., Sadjina S., Tertinek S., Dufrêne K., Pretl H., Huemer M.** A harmonic rejection strategy for 25% duty-cycle IQ-mixers using digital-to-time converters. IEEE Transactions on Circuits and Systems II: Express Briefs, 2020, Vol. 67, No. 7, Pp. 1229–1233. DOI: 10.1109/TCSII.2019.2937654

6. **Han J., Kwon K.** RF receiver front-end employing IIP2-enhanced 25% duty-cycle quadrature passive mixer for advanced cellular applications. IEEE Access, 2020, Vol. 8, Pp. 8166–8177. DOI: 10.1109/ACCESS.2020.2964651

7. **Jiang J., Kim J., Karsilayan A.I., Silva-Martinez J.** A 3–6-GHz highly linear I-channel receiver with over +3.0-dBm in-band P1dB and 200-MHz baseband bandwidth suitable for 5G wireless and cognitive radio applications. IEEE Transactions on Circuits and Systems I: Regular Papers, 2019, Vol. 66, No. 8, Pp. 3134–3147. DOI: 10.1109/TCSI.2019.2909115

8. **Ghanad M.A., Dehollain C., Green M.M.** TIA linearity analysis for current mode receivers. 2018 16th IEEE International New Circuits and Systems Conference (NEWCAS), 2018, Pp. 53–56. DOI: 10.1109/NEWCAS.2018.8585587

9. **Korotkov A.S., Tran T.D.** Optimization of current-driven passive mixer conversion gain taking into account the parameters of the low noise amplifier. 2023 International Conference on Electrical Engineering and Photonics (EExPolytech), 2023, Pp. 22–25. DOI: 10.1109/EExPolytech58658.2023.10318787

10. **Mirzaei A., Darabi H., Leete J.C., Chen X., Juan K., Yazdi A.** Analysis and optimization of current-driven passive mixers in narrowband direct-conversion receivers. IEEE Journal of Solid-State Circuits, 2009, Vol. 44, No. 10, Pp. 2678–2688, DOI: 10.1109/JSSC.2009.2027937

11. **Mirzaei A., Darabi H., Leete J.C., Chang Y.** Analysis and optimization of direct-conversion receivers with 25% duty-cycle current-driven passive mixers. IEEE Transactions on Circuits and Systems I: Regular Papers, 2010, Vol. 57, No. 9, Pp. 2353–2366. DOI: 10.1109/TCSI.2010.2043014

12. **Park J.W., Razavi B.** Channel Selection at RF Using Miller Bandpass Filters. IEEE Journal of Solid-State Circuits, 2014, Vol. 49, no. 12, pp. 3063–3078. DOI: 10.1109/JSSC.2014.2362843

13. **Luo C.-k., Gudem P.S., Buckwalter J.F.** A 0.4–6-GHz 17-dBm B1dB 36-dBm IIP3 channel-selecting low-noise amplifier for SAW-less 3G/4G FDD diversity receivers. IEEE Transactions on Microwave Theory and Techniques, 2016, Vol. 64, No. 4, Pp. 1110–1121. DOI: 10.1109/TMTT.2016.2529598

14. **Park J.W., Razavi B.** 20.8 A 20mW GSM/WCDMA receiver with RF channel selection. 2014 IEEE International Solid-State Circuits Conference Digest of Technical Papers (ISSCC), 2014, Pp. 356–357. DOI: 10.1109/ISSCC.2014.6757468

15. **Luo C.-k., Gudem P.S., Buckwalter J.F.** 0.4–6 GHz, 17-dBm B1dB, 36-dBm IIP3 channel-selecting, low-noise amplifier for SAW-less 3G/4G FDD receivers. 2015 IEEE Radio Frequency Integrated Circuits Symposium (RFIC), 2015, Pp. 299–302, DOI: 10.1109/RFIC.2015.7337764

16. **Tran T.D.** Enhanced frequency band wideband receiver using N-path Miller bandpass filter. Computing, Telecommunications and Control, 2024, Vol. 17, No. 3, Pp. 124–130. DOI: 10.18721/JCSTCS.17312

17. **Korotkov A.S., Chan T.D.** Analysis of a Current-Driven Passive Mixer at an Arbitrary Intermediate Frequency with Account of Input and Output Impedances. Journal of Communications Technology and Electronics, 2023, Vol. 68, pp. 77–87. DOI: 10.1134/S1064226923010072

18. **Nguyen T.-K., Kim C.-H., Ihm G.-J., Yang M.-S., Lee S.-G.** CMOS low-noise amplifier design optimization techniques. IEEE Transactions on Microwave Theory and Techniques, 2004, Vol. 52, No. 5, Pp. 1433–1442. DOI: 10.1109/TMTT.2004.827014

INFORMATION ABOUT AUTHOR / СВЕДЕНИЯ ОБ АВТОРЕ

Tran Thanh Dat
Чан Тхань Дат
E-mail: thanhdat140495@gmail.com

Submitted: 09.10.2024; Approved: 12.12.2024; Accepted: 13.12.2024.
Поступила: 09.10.2024; Одобрена: 12.12.2024; Принята: 13.12.2024.